International Conference on Space Optics—ICSO 2018

Chania, Greece

9–12 October 2018

Edited by Zoran Sodnik, Nikos Karafolas, and Bruno Cugny

VNIR and SWIR FPA designs for 3MI instrument: thermal, mechanical and dimensional stability challenges

Xavier Chauffleur

Gilles Marque

Antoine Weickman

Catherine Delelis

et al.

International Conference on Space Optics — ICSO 2018, edited by Zoran Sodnik, Nikos Karafolas, Bruno Cugny, Proc. of SPIE Vol. 11180, 111806S · © 2018 ESA and CNES · CCC code: 0277-786X/18/$18 · doi: 10.1117/12.2536163

VNIR and SWIR FPA designs for 3MI instrument: thermal, mechanical and dimensional stability challenges

Xavier Chauffleur*[a], Gilles Marque[a], Antoine Weickman[a], Catherine Delelis[a], Carlos Carvalos[a], Salem Belmana[a], Alain Durieux[a], Serge Primet[a]
[a] Sodern, 20 avenue Descartes, 94451 LIMEIL-BREVANNES, France

ABSTRACT

Within the framework of the 3MI instrument for METOP-SG satellite, Sodern develops the Focal Plane Assemblies (FPAs) for the SWIR and VNIR detectors. The main functions of these FPAs are the thermal cooling, the dimensional stability of the detectors and the mechanical withstanding with respects to the thermal and mechanical environments. From a mechanical point of view, the mechanical requirements are identical for the two FPAs with notably stiffness above 500Hz. On the other hand, from a thermal point of view, the temperature environment and thermal control principle between SWIR and VNIR FPAs are different by the use of a heater for SWIR and a TEC for VNIR. At last, the SWIR FPA turns out to be the more challenging case with a high insulation, up to 200K/W, between cold parts (-90°C) and hot interface (25°C) and also a high coupling of 2.7K/W with the cold sink. This paper shows how a single architecture composed of a hexapod structure made of 6 titanium shafts and a thermal strap made of low diameter copper strands permits to achieve the best compromise between thermal and mechanical requirements for both FPAs. In addition to technical aspects, this common architecture also answers to the aim of cost cutting for the different phases of the project: design sharing, grouping of supplies, mutual qualification tests, shared integration tools and processes. Several models have been integrated and tested to verify the performances and the withstanding to thermal and mechanical environments.
Keywords: 3MI, FPA, SWIR, VNIR, hexapod, thermal control, dimensional stability

1. INTRODUCTION

MetOp-SG (Meteorological Operational Satellite - Second Generation) is a series of six meteorological satellites developed by the European Space Agency and EUMETSAT to be deployed in orbit from year 2021 (see [1]). With 10 different instruments, covering the ultra-violet, visible, infrared and microwave spectral bands, MetOp-SG will provide continuity and enhancement of meteorological data with improved spectral and spatial resolution compared to that currently provided by the first generation of MetOp satellites.

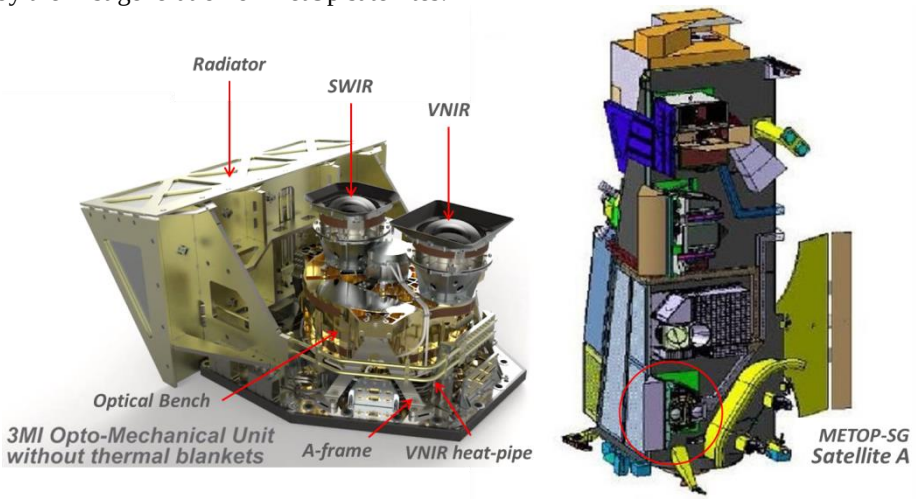

Figure 1. View of METOP-SG with 3MI implantation and 3MI instrument.

*xavier.chauffleur@sodern.fr; phone +33 (0)1 45957179; sodern.com

The 3MI (Multi-Viewing Multi-Channel Multi-Polarization Imaging) instrument will be used for Earth observation in a multiplicity of conditions, varying spectrally (410 - 2130 nm), polarization (-60°, 0°, +60°) and viewing angles (14 different views of the same target area). 3MI is designed for aerosol observation and it will greatly support the observation of Earth radiation budget, clouds microphysics, soil condition and ocean color.

Under the responsibility of LEONARDO Company in Florence, the design of the 3MI instrument is composed of 2 optical modules, namely VNIR and SWIR. These two modules are mounted, in a diametrically opposed way, on a circular optical bench, itself mounted on a CFRP baseplate by means of 3 bipods. The optical bench also supports a common filter wheel with two coaxical rows of filters for each optical module. A module is composed of an optical channel and a detector (Detector Unit) mounted on a FPA (Focal Plane Assembly). Sofradir and e2v are in charge of the SWIR and VNIR detectors respectively, while IberEspacio provides a radiator to cool down the two FPAs.
Each FPA is connected to a dedicated FEE (Front End Electronic) by means of a flex cable. This electronic manages the digitation of the images and the thermal control loop of the detector. It also provides interfaces to both nominal and redundant ICU (Instrument Control Unit). The TM/TC and digitized video data are managed through Space Wire interface. The housing of this electronic is mounted on the CRFP through an aluminum interface plate.

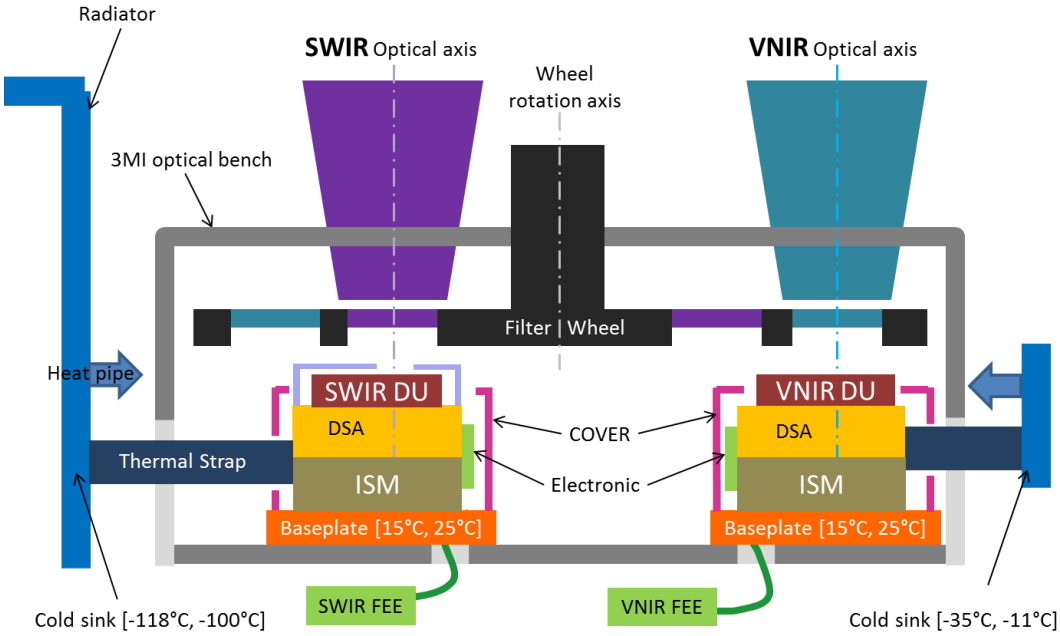

Figure 2. Schematic representation of FPAs into 3MI instrument.

For both SWIR and VNIR, a FPA is composed of:

- the DU (Detector Unit);
- a baseplate as mechanical interface with the 3MI optical bench;
- an ISM (Iso Static Mounting) to insure the dimensional stability of the detector under mechanical loads during launch and temperature variation during operative mission;
- a thermal strap for the thermal cooling of the detector;
- a DSA (Detector Support Assembly) as mechanical and thermal interface between the detector and both ISM and thermal strap and also as support of the proximity electronic boards;
- a proximity electronic for the management of the detector;
- a cover for thermal radiative insulation and handling protection;
- for SWIR, a cold shield for thermal radiative insulation with an optical aperture for parasitic light protection.

Each SWIR and VNIR thermal strap is linked to a specific cold sink. For SWIR, the cold sink is directly the radiator. For VNIR, located opposite to the radiator, a heat-pipe is used between the radiator and the VNIR cold sink.

2. SPECIFICATIONS

2.1 Thermal

The active area of the detectors must be cooled down in order to reduce the parasitic noise. Apart from the packaging made of Kovar, the SWIR and VNIR detectors are different for many aspects such as the light spectrum range and thermal management.

For the SWIR detector, the operating temperature of the chip is 185K. The cooling down to this operative temperature is simply achieved by conduction through the backside of the package. Two transistors are glued into the package and are used as thermal sensors in order to read and / or control the temperature of the detector.

For the VNIR detector, the electro-optic technology is based on CCD. The chip is composed of an active and storage areas mounted on a ceramic layer. Two thermal sensors are also glued on this ceramic layer to read and / or control the temperature of CCD at -20°C in order to reduce the noise. Unlike the SWIR detector, the cooling down to this temperature is achieved by a two stages Thermal Electrical Cooler (TEC) directly integrated into the detector package. So the FPA shall cool down the package of the VNIR detector that will be hotter than the chip.

The FPAs are thermally coupled with the 3MI instrument through three thermal interfaces (see figure 2):

- radiative environment;
- conduction at baseplate I/F;
- conduction at cooling I/F.

The radiative environment and baseplate I/F are identical in term of range and defined as imposed temperature covering hot and cold cases. A low emissivity surface (0.1) is specified for radiative environment.

The definition of the cooling I/F is more complex. Instead of an imposed temperature, the temperature of this I/F is defined as a function of the power rejected by the FPA. This function takes into account the performance of the radiator and the heat pipe in the case of VNIR FPA. Thanks to this method, the operation point of the FPA can be easily simulated without the need to iterate with thermal engineering at upper system level. As the function between temperature I/F and rejected power is linear, the thermal performance of the radiator can be modeled by a reference temperature defined for a null rejected power and a thermal resistance.

The following table sums up the value of the temperature I/F.

	Case	Baseplate	Radiative	Cooling	
		Temp. (°C)	Temp. (°C)	T ref (°C)	Thermal resistance (K/W)
SWIR	Cold	15	15	-118	3.4
	Hot	25	25	-100	3.6
VNIR	Cold	15	15	-35	6.6
	Hot	25	25	-11	6.2

Table 1: Summary of thermal I/F.

The FLEX cable between the FPA and the FEE also represents a thermal interface by mains of:

- conduction due to the thermal gradients between these two parts;
- radiative exchange of the flex cable with the instrument environment.

The thermal flux transmitted by this part will be managed by design in order to have a negligible impact of the temperature of the DU.

The maximum power dissipation of the detectors and the maximum power available for the thermal control are indicated in the following table.

	Detector dissipation	Thermal control budget
	(W)	(W)
SWIR	0.18	3 for heater
VNIR	0.14	2 for TEC

Table 2: Detector and thermal control maximal power.

2.2 Mechanical

The main mechanical requirements for both FPAs can be divided into the following items:

- The first eigenfrequency of the FPA must be above 500Hz in order to avoid dynamic couplings with the instrument;
- the stability of the detector interface with respect to the baseplate mechanical reference for optical performances. It must be less than ±1µm for the in-plane direction, less than ±4µm for the out-of-plane direction and must take into account gravity release, mechanical and thermal environments (tests, launch and operative), relative displacement of ±1mm in any direction of the thermal strap (the total displacement is ±3.5mm taking into account ±2.5mm of ground alignment during instrument AIT);
- the level in random vibration and shock at detector interface to avoid any degradation respectively 51gRMS and SRS level of a half-pulse of 1500g, 0.5ms above 1500Hz corresponding to the lower frequency mode of the detector;
- the equivalent Quasi-Static Load in random vibration to limit the load with instrument interface;
- the mass of the FPA: lower than 0.72kg for SWIR and 0.65kg for VNIR excluding DU mass (around 0.125kg);
- the Interface Requirement Document (IRD) with in particular the space for the FPA and the positioning of the detector.

Stiffness, thermal regulation, dimensional stability and IRD are the main design drivers that will be discussed in details in this paper.

Random vibrations and shocks loads are also challenging but can be managed by iterations with mechanical engineering at upper system level thanks to notching approach or level update ([5]).

3. DESIGN

3.1 General considerations

The design of a FPA, like most of the opto-mechanical devices and in particular in space applications, is a complex task because the specifications are numerous, with a high level of accuracy (temperature and dimensional stability) that must face severe environments. These specifications, especially mechanical and thermal ones, lead to conflicting solutions. A tighten optimization in the choice of materials, architecture and dimensioning is needed to overcome any stalemate.

The project addresses the development of two FPAs. SWIR and VNIR specifications are identical or very close from a mechanical point of view but opposite in term of thermal specifications:

- the operating temperature of the SWR and VNIR are widely different, respectively -88.15°C and -20°C;
- the principle of thermal regulation is based on heater for SWIR and on TEC for VNIR.

Despite these technical challenges and differences of specifications between SWIR and VNIR FPAs, the development of a specific solution for each of these two FPAs is to be avoided because it will lead to additional costs and time delays. Therefore, the strategy is to develop one FPA and adapt the resulting design to the other FPA. This approach during the developing phase is also beneficial for the following phases: common parts lead to reducing purchase costs and delays, similarity of product design is reflected on tools and methods for integration and testing.

SWIR FPA appears to be more dimensioning in comparison to VNIR FPA. Without any computation, the thermal specifications show that the design is out of the state of the art. For SWIR, the detector must be at a temperature lower than -88.15°C with a temperature of thermal sink at -100°C that represents a thermal gradient of 12°C that is lower than usual margin of 15°C (5°C for analysis uncertainties, 5°C for acceptance and 5°C for qualification as defined in [3] and [4]). On one hand, this small gradient implies to have a high thermal coupling. On the other hand, the thermal gradient with the baseplate is very high, up to 133°C, thus implying to have a high insulation to avoid too much thermal losses.

3.2 Materials

The choice of materials is a key step in the design process because it implies to take into account many compromises:

- a high mechanical strength especially regarding shock;
- a high thermal conductivity in order to cool down the detector and low thermal conductivity to reduce the losses with hot parts;
- a low CTE for dimensional stability or at least matching CTEs between parts to avoid sliding at an interface.

Silicon Carbide is widely used in FPA structures because of its dimensional stability: it's a rigid material with low deformation under thermal loads thanks to a high thermal conductivity to reduce thermal gradient and also with a low CTE. The latter property is usually compatible with the detector material. The main drawback of this material is its fragile behavior under shock.
In addition, with the low temperature range specified for SWIR FPA, only a DSA made of Kovar, i.e. identical to the detector package, is suitable to avoid sliding at screws interface. Flexible items could be used to relax thermal elastic efforts but they are not compatible with high eigenfrequencies requirement, thermal coupling and also the lack of room allocated by the IRD.

For similar reasons, 6082 aluminum alloy is used for the baseplate and for the end of thermal strap in interface with the 3MI instrument. The thermal treatment is basically T6 but, to face the reduction of thermal conductivity at low temperature observed on aluminum alloys, a O temper is defined for the thermal end (see §3.6 for details on thermal strap).

The most critical part of the FPA remains the ISM because it must insure its thermal insulation and mechanical stiffness. These two functions can be realized by separated parts. For example, ceramic washers are widely used as local thermal insulators. But, after a detailed analysis, they don't provide any advantage in comparison to shaped titanium parts: higher volume and mass at identical thermal resistance, fragile materials with risks of failure during assembly phase and environment loads, the need of additional washers for thermal-elastic compensation of screws tightening, an increase in the number of parts, an increase in the complexity of assembly phase. Some composite materials, fibers encapsulated into resin, have also been foreseen because of their low thermal conductivity and their relative stiffness but their stability with respect to humidity absorption and creeping over time storage of satellite before launch are not compatible with dimensional stability.

Finally, titanium alloy and more precisely TA6V is chosen because it represents the best material for all the constraints presented above. However, this choice must be completed by the geometry of the ISM to reach all the performances.

3.3 Thermal budget

The global thermal budget of the FPA can be generalized by the following figure where the temperature of the DSA is a function of temperature and thermal resistance at the two interfaces:

- T_{sink} is the cold interface associated with R_C, resistance of cooling;
- $T_{baseplate}$ is the hot interface associated with R_L, resistance of losses.

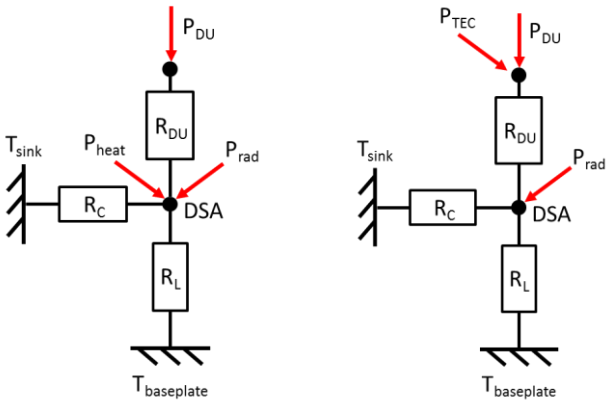

SWIR configuration VNIR configuration

Figure 3: Global thermal models of FPA.

This figure shows the main difference between SWIR and VNIR FPA:

- in the case of the SWIR FPA, the thermal control is located at DSA level and is active in cold case to warm-up the detector;
- in the case of the VNIR FPA, the thermal control is located at the detector level and is active in hot case to cool-down the detector. As the power of the TEC is injected into the detector package, the thermal resistance of this item is more sensitive than for the SWIR detector package.

In this model, the thermal flux brought back by the flex cable to the FPA can be neglected because:

- by hand computation, this flux remains low (less than 0.1W);
- by design, the flex cable is fixed to the baseplate in order to secure the interior inter-connections from exterior efforts during manipulations, this flux is directly driven to the baseplate I/F and not into the FPA and notably to the DSA.

Based on this model for the SWIR FPA, the following equation gives the relationship between the DSA temperature according to the cooling and losses thermal resistances, the interface temperature of the cold sink and the baseplate.

$$\frac{T_{sink} - T_{DSA}}{R_C} + \frac{T_{baseplate} - T_{DSA}}{R_L} + P_{heat} + P_{DU} + P_{rad} = 0 \qquad \text{Eq. 1}$$

The power of radiative coupling with the environment is hand-computed and remains low if parts are treated with low emissive coating like gold or SurTec. The desired temperature of the DSA is computed from the detector characteristics (operating temperature, resistance of the package and its assembly and the dissipated power):

$$T_{DSA} = T_{DU} - R_{DU} \times P_{DU} \qquad \text{Eq. 2}$$

Taking into account the fact that equation Eq. 1 is applicable for hot and cold cases with, in particular, a null value of heating power in hot case, the values of the cooling and losses resistances can be determined and used as derived specifications for the design guide line:

$$R_C = 6.23\ K/W\ ,\ R_L = 88\ K/W$$

The range of magnitude of these resistances confirms that the DSA must be highly coupled with the cold sink and highly isolated from the baseplate to limit the losses. It is due to the fact that the temperature of the DSA (-89°C) is very close to the cold sink in comparison to the baseplate. As the resistance of losses is very high, the power dissipated by the heater is directly injected to the cold sink, it can be observed that the resistance of cooling corresponds to the compensation of the temperature variation of the cold interface between hot and cold cases: 6.23K/W x 3W = 18.69°C ≈ 118°C – 100°C. It also means that the need of heating power can be reduced if the resistance of cooling is increased but with the drawback to also increase the losses resistance to maintain the equilibrium in hot case.

Each of these two resistances is also derived into two resistances:

- the resistance of cooling is composed of the resistance of the cold sink in series with the resistance of the thermal strap that must be 2.7K/W for a mean thermal resistance of the cold sink equal to 3.5K/W;
- the resistance of the losses is composed of the resistance of the ISM in parallel with the electrical flexes for the control of the detector. The objective value for these two thermal resistances is determined at 200K/W for a total resistance of 100K/W corresponding to R_L with at least 10% of margin.

3.4 Thermal and mechanical optimization of ISM

Form this primary analysis and specification, the ISM must respond to two opposite objectives:

- have a high thermal resistance of 200K/W;
- have a high stiffness of 500Hz.

As already discussed, Ta6V titanium alloy is identified as the best material for this type of application. The important challenge is now to find the optimal geometry to achieve these objectives. Thermal insulation requests to design parts with a reduced cross-section and an increased length while stiffness requirements lead to the opposite.

The DSA, as well as the detector, also play a role in the stiffness performance of the FPA because they represent the major part of vibrating mass, notably by the fact that they are made of Kovar. Nevertheless, these items cannot be thoroughly optimized. Firstly, the mass of the detector is an imposed input data. Secondly, the size of the DSA and then its mass is constrained by two parts in interface with it: the detector and the thermal strap.
However, a significant parameter is the location of the fixing of the thermal strap on the DSA. Basically, two options are possible: as the cold sink is located on the side of the FPA, either a part of the DSA passes through the ISM to join the thermal strap or it's the thermal strap. During design tread-off, the first option has been chosen but the second one appears to be the best for many reasons:

- the thermal conductivity of the Kovar is lower than the thermal strap so the length of the kovar must be minimized to reduce thermal gradient;
- the density of the Kovar is more important than the one of thermal strap and any mass located far from the center of gravity creates a balancing mass that lowered the frequency eigenvalues.

In addition, as the thermal strap is a flexible part (see §3.6), its resonance frequencies are very low (around 50Hz) in comparison to stiffness requirement and its mass does not bring in account the effective mass of the FPA design.

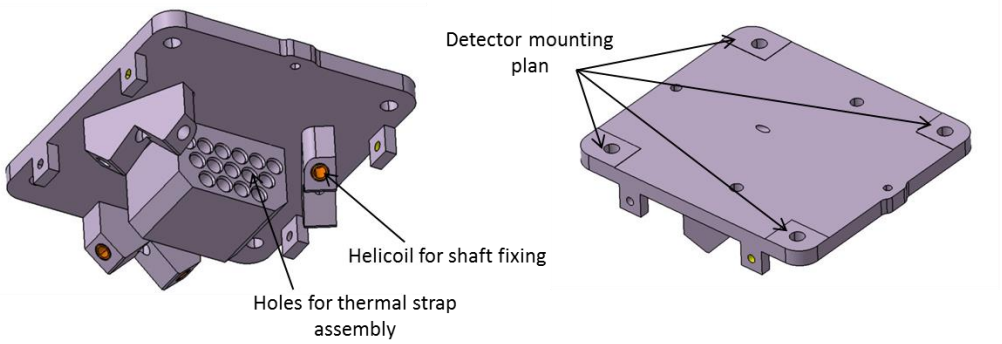

Figure 4: Final design of the SWIR DSA.

The VNIR DSA is adapted from SWIR DSA to take into account the difference of detector interface and electronic boards.

The method to optimize the thermal and mechanical design of the ISM is based on two steps:

- define a principle of architecture;
- parametrize the dimensions of this architecture (length, diameter, thickness) and perform a design optimization based on the two criterion (maximize thermal resistance and first frequency mode).

The following figure shows the different architectures that have been envisaged.

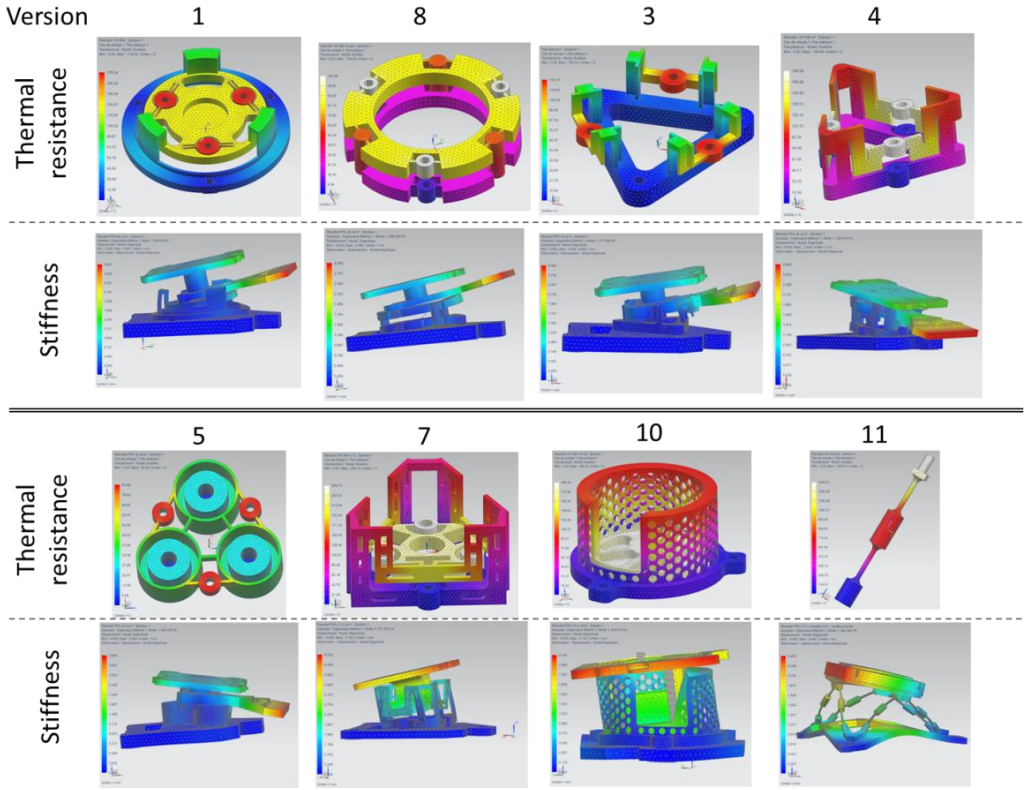

Figure 5: Some of the explored architectures for ISM.

The results of this optimization phase are analyzed by means of a Pareto diagram (figure 6). On this diagram, each iteration is represented by a point which stiffness is reported on the horizontal axis and the thermal resistance on the vertical axis. To be compliant, an iteration must have its representing point located in the white area: Rth > 200K/W and freq. > 500Hz. The points having the same color correspond to the optimization of one architecture.

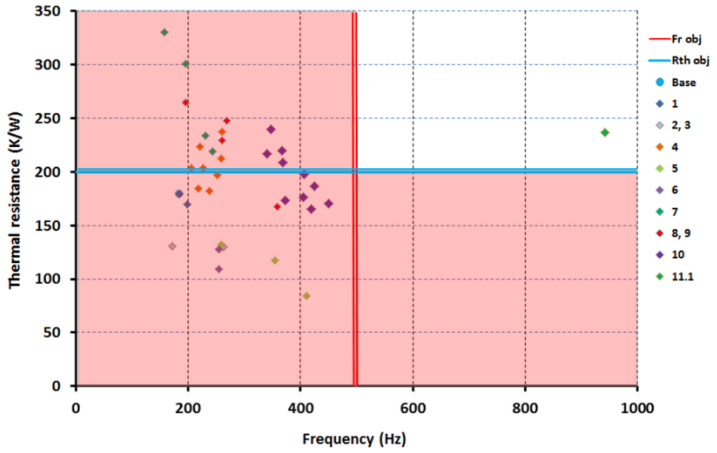

Figure 6: Pareto diagram of stiffness and thermal resistance objectives.

The Pareto diagram shows that the only architecture capable to fulfill the thermal and stiffness requirements is the number 11.1 corresponding to a hexapod composed by 6 shafts. This architecture is an extrapolation of a trivial hexapod used to sustain large structures like mirrors of telescope or other optical devices ([6], [7], [8]).

This architecture offers other advantages:

- the room between the different shafts permits to arrange a passage for the thermal strap;
- the ideal angle between two shafts is 110° to obtain an isostatic stiffness (same stiffness in all directions). For stability purpose, this angle is modified in order to compensate the thermal expansion of the shafts (see §3.5);
- unlike bipods or A-frame where the axis of the beams is not aligned with the interface plans, the shafts are mounted on angled bearing surfaces. As the shafts are flexible in bending and only transmit tensile/compressive loads, no shear effort is transmitted to interface with the bearing surfaces that avoid any sliding of the assembly.

The direct drawback of this latter advantage is that angled surfaces must be manufactured with a high accuracy (50µm to 10µm) to limit the initial stresses during the mounting. Special tools are designed to secure the shaft, notably to counteract the torque during the tightening of the screws.

In the final optimization, buckling is also taken into account as dimensioning criteria because shafts are slim structures ([9]). Equivalent load to maximum RMS acceleration acceptable by the detector and a safety factor of 10 is considered to cover the uncertainty of linear buckling analysis.

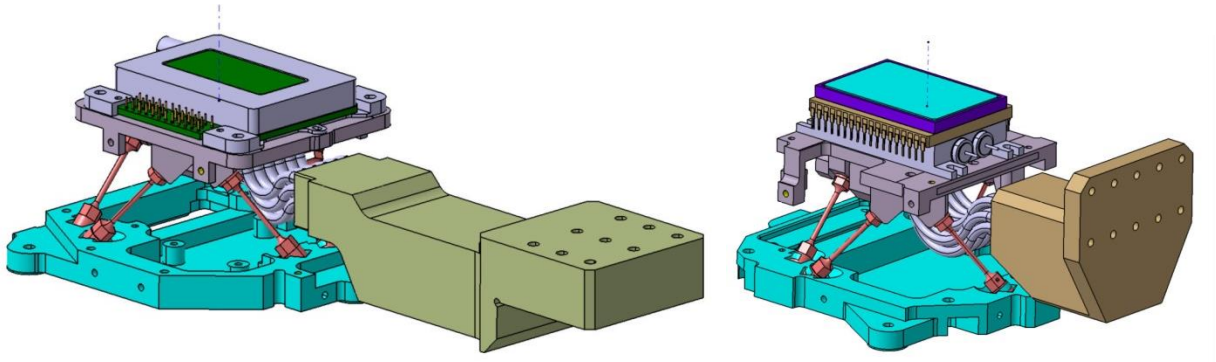

Figure 7: View of SWIR and VNIR hexapods with thermal strap.

On the figure 7, one can notice that the fixings of the shafts on the SWIR baseplate are aligned with the fixings of the baseplate on the 3MI instruments. It allows avoiding any contribution of the stiffness of the baseplate. Unfortunately, the application of this design rule is not possible for VNIR baseplate and we observed a lower stiffness of the VNIR FPA (620Hz) in comparison to SWIR FPA (798Hz).

3.5 Thermo-elastic dimensional stability

The in-plane stability can be easily managed if the whole structure is symmetric and aligned around the optical axis of the optical bench:

- the optical axis of the detector is aligned with the optical bench while it is not centered with its package;
- each of the three sets of two shafts are arranged at 120°;
- the IRD is modified to insure that the three fixing points of the baseplate on the 3MI instrument form an isosceles triangle.

The fact that the optical axis of the detector is not aligned with its package creates an unwanted shift of the center of gravity of the vibration mass that penalizes the dynamic behavior by rotations of the DSA and then an increase of amplifications factors.

The out-of-plane stability is more complex because the architecture must be able to compensation the thermal expansion of the materials in order to maintain the detector at the same distance from the baseplate.

Some of the architectures presented in **Błąd! Nie można odnaleźć źródła odwołania.** are designed with an ISM having a 'round trip' shape along the thermal path. The vertical expansion of the forward path is compensated by the expansion of the backward path. If the lengths of the two paths are not identical, their cross-sections must be adjusted to distribute their respective thermal gradients with a ratio inversely proportional to the ratio of the lengths. With this architecture, the thermal gradient within the DSA must be negligible that implies the use of material like SiC instead of Kovar.

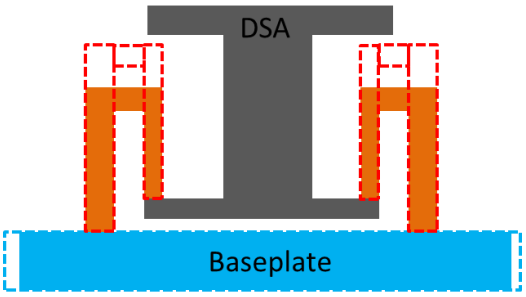

Figure 8: Out-of-plane dimensional stability behavior of FPAs with 'round trip' principle.

This principle is not feasible with a hexapod at least within the room allocated by the IRD.

The vertical compensation of hexapod is obtained by a more complex kinematic. When the temperature increase, two phenomena occurs:

- the baseplate inflects in the plane, the distance between the fixing points of the shafts increases, the triangle forms by two shafts caves in and the DSA goes down;
- on the contrary, the length of the shaft increase and the DSA goes up.

An optimization of the angle of the triangle forms by two shafts permits to adjust the two phenomena to obtain a perfect compensation.

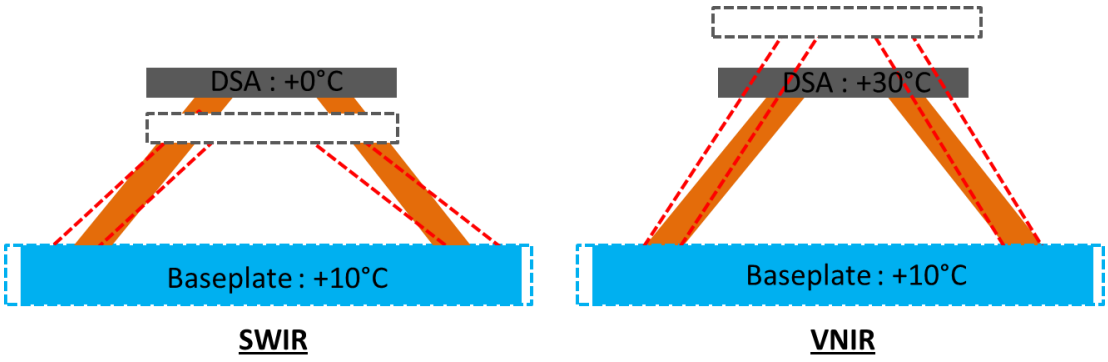

Figure 9: Out-of-plane dimensional stability behavior of SWIR and VNIR FPAs with a hexapod.

The mean temperature variation of the shafts is the median of the variations of the baseplate and the DSA. As the thermal control is different between SWIR and VNIR FPA, the variations of temperature of the shafts are not the same for the two FPAs (see figure 9):

- with a thermal control with heater at DSA level, the temperature of the DSA is stable;
- with a thermal control with TEC at detector level, the temperature of the DSA varies according to the thermal resistance between the DSA and the cold sink and rejected power by the TEC and the electronic of the detector.

However, in order to keep a common design between SWIR and VNIR, a correction is not complete and a compromise is established. The relative displacement of the DSA is:

- +1.35µm for SWIR;
- -2.45µm for VNIR;

for a temperature change of between median case and hot case.

3.6 Thermal strap

An important tread-off has been carried-out in order to realize the thermal strap with the following criteria:

- the stiffness and the thermal resistance for performances;
- the size including the ends to face the arrangement into the IRD and FPA itself;
- the capacity of integration with the mechanical structure;
- the cleanliness;
- the price.

The stiffness of the strap must be taken into account when dimensional stability is needed like for FPA devices. The relative displacement of the thermal strap produces a displacement of the DSA proportional to the ratio between the stiffnesses of the thermal strap and the ISM: 40 to 150N/m for transverse directions and 2500 to 3500N/m for direction along the length of the strap depending on SWIR or VNIR FPA. Tests on samples and hand-computations based on beam theory demonstrate that the flexibility for this latter direction is mainly tunable according to the shape of the strap: an important loop promotes more flexible bending deformations compared to traction/compression.

Three different thermal strap technologies are described hereunder:

- copper braid technology: this is the most standard design offering a limited envelope volume with a good thermal conductivity in comparison to aluminum. The mechanical flexibility depends on characteristics of the braids and notably on the diameter of the strands. Sodern typically uses braids woven with 150µm-diameter strands. To improve the flexibility, strap with 50µm-diameter strands is preferred: at equal thermal performance, these braids are expected to be 10 times more flexible. Samples have been supplied and confirm the fact that braids with smaller strands are more flexible;
- copper or aluminum foils technology is a spatial common design also. Copper foils offer an envelope volume smaller than copper braids, but transverse flexibility is not guaranteed without smart rotation of the strap;
- graphite braids technology is an emerging technology. Two different technologies have been identified:
  - thermal straps made with graphite fiber. This product offers a slightly improvement of the thermal performance and none advantage concerning the stiffness. The main advantage is the reduction of weight;
  - the other technology is thermal straps based on pyrolytic graphite encapsulated into aluminum sheet. These straps offer better performance for nearly of fields (thermal performances, flexibility and weight).

  The main drawback for both technologies is the price that is 6 to 8 times more expensive that a standard copper strap without including the cost of specific prototypes needed during the development of the product (few space heritage and maturity of both technologies).

Finally, copper braid technology is retained for its capability to be directly integrated into the structural parts of the FPA, without intermediate ends. It allows a reduction of volume, weight and no contact thermal resistance at connection. The connection between the strap and the structure is a key point, whatever is the retained technology. For 3MI FPA, a special technology is developed with FORISSIER company: a silver tube is crimped around the braid (see figure 10). It facilitates the insertion of the braids into the holes of the mechanical parts and permits a better control of the thickness of the joining material. In replacement of solder initially envisaged, a glue, specifically designed for cryogenic applications (CTE closed aluminum, low outgassing), is used to maintain the braids into the mechanical parts.

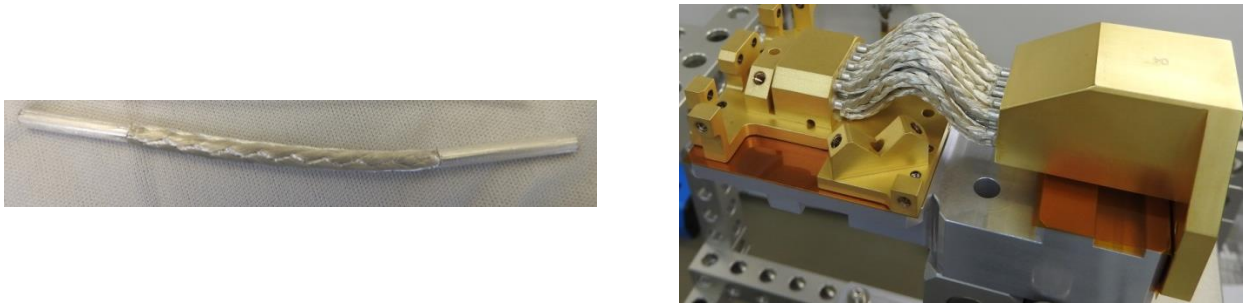

Figure 10: VNIR braid with silver tubes at each end and assembly (DSA, braids and thermal rod) during AIT.

For thermoelastic reasons, the end of the strap in contact with the 3MI instrument (named thermal rod) must be made of aluminum. A special attention is paid to the choice of the grade and thermal treatment because one can observe a decrease of the thermal conductivity at low temperature for many of them ([10]). The best compromise found between thermal and mechanical performances is the grade 6082-O.

3.7 Gluing of detectors

Thermal resistances of detector package are indicated with in ICD but are only applicable if package is in thermal contact on the whole area of the back side of the package. In the early design, the detectors were only fixed on the DSA by 4 screws. In this case, the thermal exchanges between the DSA and the detector can only be achieved at the 4 corners. As a result, the assumption declared in the ICD was not obtained and the thermal resistance of the detector package was much more important, 27K/W instead of 0.9K/W, especially as the package is made of Kovar that is a low thermal conductive material. In addition, the same phenomenon occurs in the DSA because of the distance between the corners and the center where the thermal strap is fixed (see figure 11).

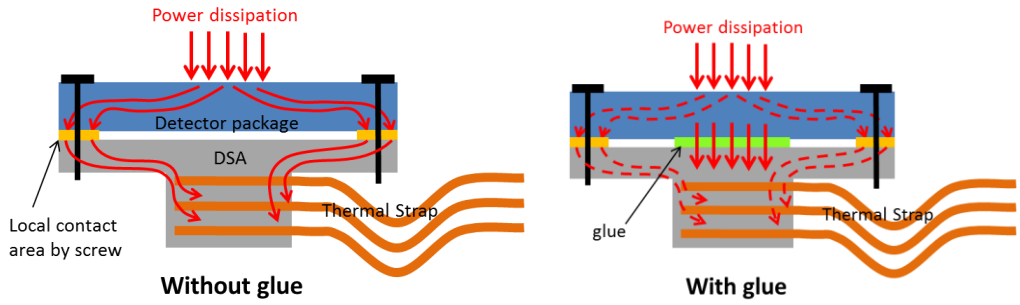

Figure 11: Addition of glue to avoid gradients in detectors and DSA.

The solution to shorten the thermal paths consists by adding a Thermal Interface Material, TIM between the detector and the DSA. The criterion used to choose this TIM takes into account thermal performances but also mechanical aspects:

- pre-load during integration needed to insure a satisfying contact;
- load due to thermo-elastic effects;
- long term storage.

The loads criterion mentioned above concerns the screws used to fix the DU on the DSA and also those applied to the DU. Even if no specific limit is mentioned in the ICD of the DU, Sodern looks for TIM allowing a limitation of the efforts transmitted to the DU. In the sense, elastomer or soft metallic layers are rejected. The usage of a glue identical to the one retained for the thermal strap is the best candidate. Qualification process to verify the adhesion on gold coating is still in progress.

3.8 Electronics integration

In §0, the thermal resistance of the flex cable of SWIR detector must be higher the 200K/W. With respect to electronic signals performances, the flex are designed with the following guide lines:

- the thickness of the copper layers are limited to 17µm;
- the width and the length of the tracks are optimized with electrical impedances;
- only one layer of EMC protection is designed. This layer is a grid facing the exterior of the FPA.

The space left for the integration of the proximity electronic is very small because of the size of the detectors in comparison to the space defined in the IRD. The electronic boards and flexes are shaped to pass around the 6 shafts of the hexapod and fixed on the DSA.

4. MODEL VALIDATION

4.1 Mechanical tests

AMM, Advanced Mechanical Model

Early mechanical models are realized in order to:

- verify the mechanical strength of the hexapod structure;
- characterize the damping in random vibration for notching determination;
- determine the amplification factors under shock;
- verify the dimensional stability.

Notching is defined to limit the acceleration in random vibration and shock at detector interface, respectively 51gRMS and 1250g, half-sine during 0.5ms finally converted into SRS.

A ballast is designed and mounted on the DSA in order to represent the mass of the detector and the proximity boards.

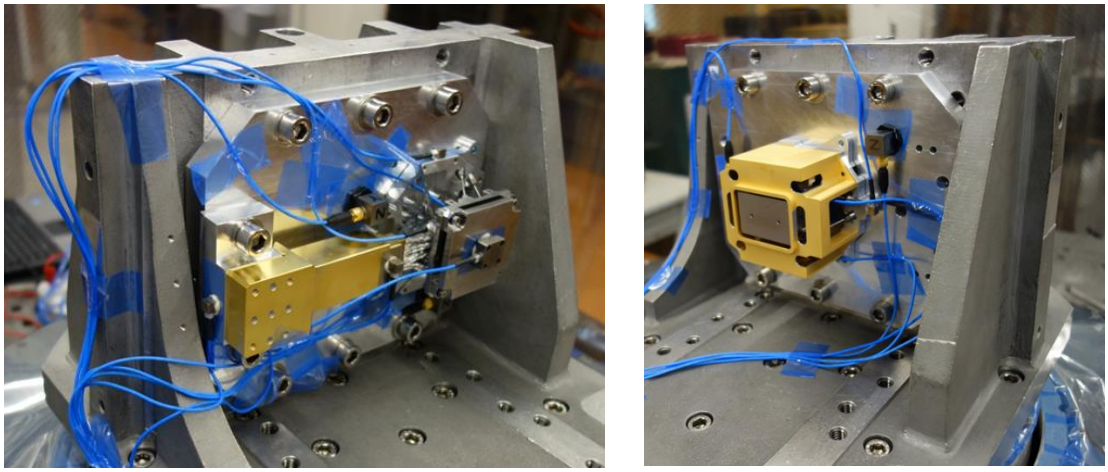

SWIR FPA AMM VNIR FPA AMM

Figure 12: Views of SWIR and VNIR FPA AMMs (configuration for tests in X axis).

Tests performed with SWIR FPA AMM shows that the thermal strap has no influence on dynamic behavior of the FPA, whatever is in terms of stiffness or damping. For this reason, no thermal strap is mounted on VNIR FPA AMM.

The table 3, figure 13 and figure 14 show that the FEMs can correctly predict the mechanical behavior of the FPAs that are relative simple structures. The measured amplification factors are more important than expected: from 40 to 190 according to the frequencies modes and direction.

mode	f tests (Hz)	f FEM (Hz)	Q (LSRC)	Q (random)
first Y	791	793	74	54
first X	815	804	125	85
Z (front)	1017	987	45	55
Rotation Y	1268	1214	40	40
Rotation Z	1307	1259	212	135
Z (back)	1344	1352	100	40

SWIR FPA AMM

mode	f tests (Hz)	f FEM (Hz)	Q (LSRC)	Q (random)
first X	606	654	102	88
first Y	648	651	57	77
Z	1017	973	66	63
Y/Z	1452	1391	110	130
second X	1663	1583	280	190

VNIR FPA AMM

Table 3: Eigenvalues and amplification factors measured on SWIR and VNIR AMMs.

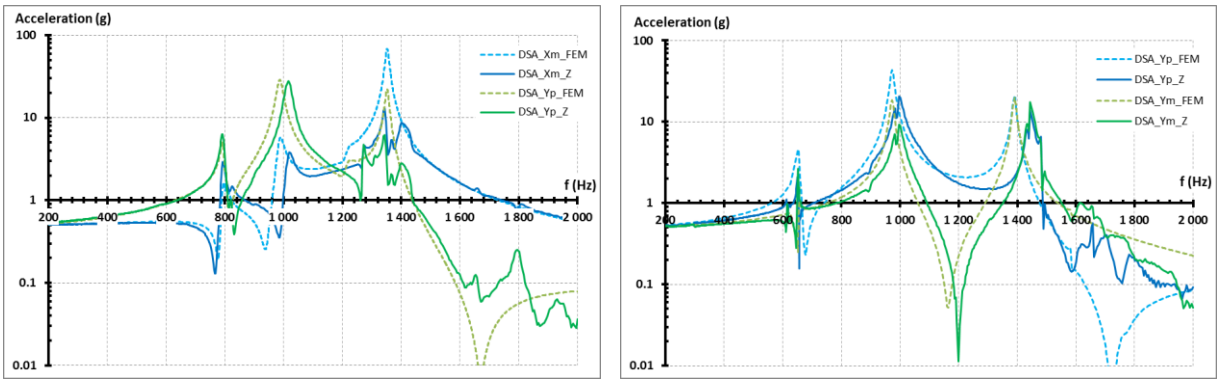

SWIR FPA AMM VNIR FPA AMM

Figure 13: Comparison of measured and computed LRSC in Z axis between AMM and FEM.

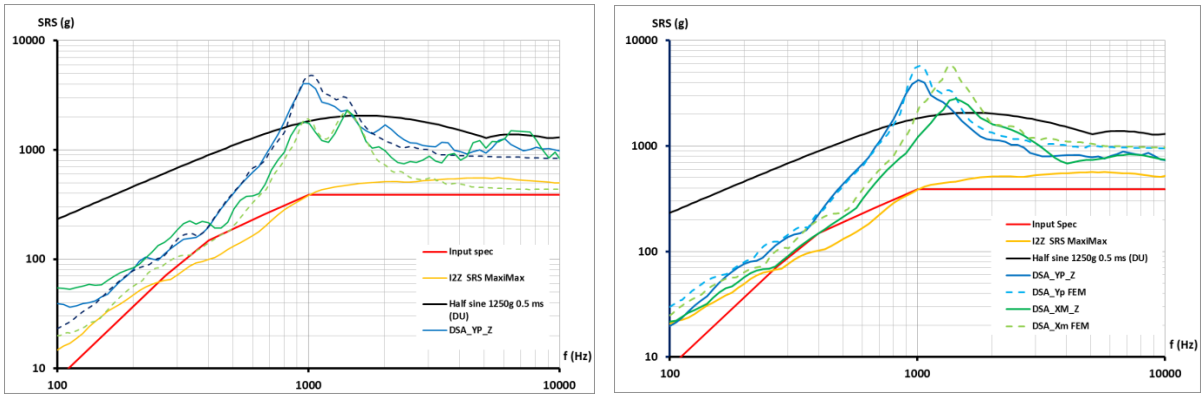

SWIR FPA AMM VNIR FPA AMM

Figure 14: Comparison of measured and computed shock responses in Z axis between AMM and FEM.

Even if the output SRS levels exceed the maximum level of detector for frequencies close to the resonances of the FPAs (1000Hz), these levels are acceptable because they are below this limit for frequencies above 1500Hz corresponding to the first frequency resonance of the detector.

STM, Structural and Mechanical Model

The first aim of the STM is the validation of the thermal performances (see §4.2). For this reason, functional detectors are mounted on the FPA in order to have a full representation of their thermal behaviors: power dissipation of detector and proximity electronics, dissipation of the TEC for VNIR, losses by the flex cables, measures of temperature of sensing elements.

Mechanical tests on STMs confirm the dynamic behavior observed on AMMs.

The main interest of the STM mechanical tests campaign is the measurement of the dimensional stability with respect to the mechanical and thermal environments including operational and non-operational conditions. A set-up of these measurements is performed in order to quantify and reduce as much as possible the accuracy. 3D machine programing, positioning of the sample and statistical approach permits to reach an accuracy of ±2µm. Apertures in the cover of the FPAs are tooled in order to allow the access of the sensor to the DSA and the detector and the outlet of accelerometer cables.

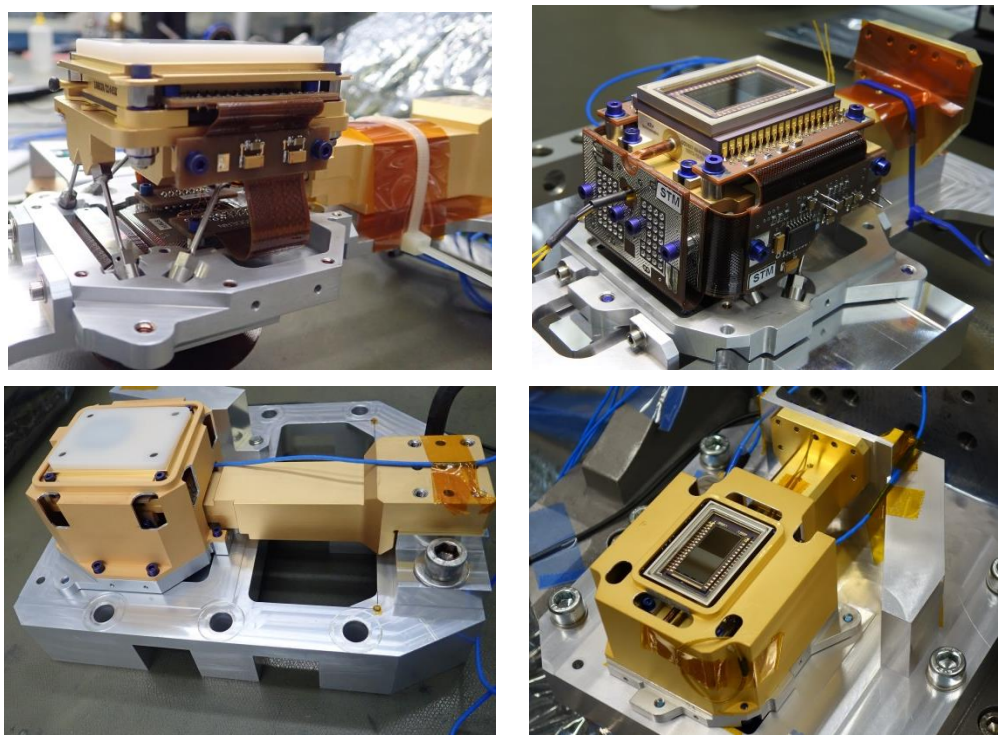

SWIR FPA STM VNIR FPA STM

Figure 15: Views of SWIR and VNIR FPA STMs.

After each environment, a series of measurements with the 3D machine are performed. The mean value and the standard deviation of the series are computed and are reported on the following graphs:

- the solid bar represents the difference of mean positions between at a given environment and the reference;
- the thin bar represents the standard deviation of the considered series of measurements.

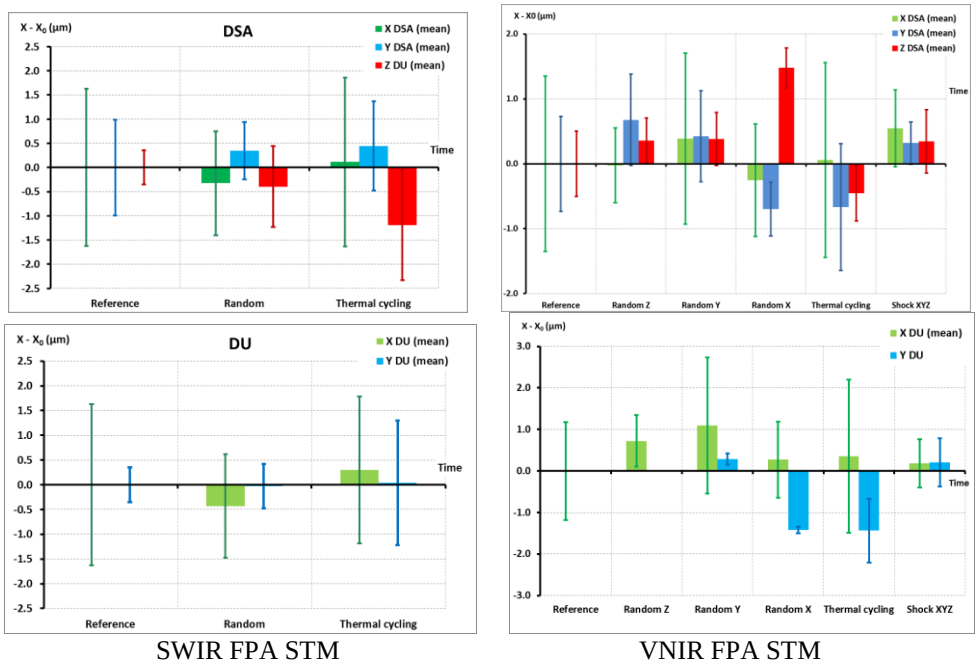

SWIR FPA STM VNIR FPA STM

Figure 16: Results of dimensional stability measurements after random, thermal and shocks environments.

From these data, we observe that no permanent deformation or sliding occurs during vibration, shock and thermal tests:

- the main value of displacements are always lower than the 3D machine accuracy;
- most of the time, this observation is also verified when we consider the sum of the mean value and the standard deviation;
- all along the sequence of tests, no progressive displacement is observed (the sign of displacement is erratic) that would not have been observed if real sliding occurred;
- for a given time step, the in-plane displacements of the DSA and the DU are in the same direction that means that no sliding occurs at the mounting I/F of the DU.

4.2 Thermal tests

Thermal Vacuum Equipment

In comparison to standard thermal tests, the particularity of the FPA tests is the fact that the cold sink interface temperature is not fixed value but must be representation of the linear variation with rejected power (see table 1). The implementation of this specification is realized by the design of aluminum rod with the appropriate length and cross-section. Even with a 3D FEM analysis, the thermal resistance must be measured in order to recover uncertainties mainly due to the thermal conductivity decrease at low temperature. In addition, the residual error with the specification must be corrected with the adjustment of the detailed thermal model in order to determine the thermal performance of the FPA in specified environment.
Despite of the difficulties encountered to implement this specification, an advantage is the capability to measure the power rejected at the interface. It allows to validate the performances of the device in terms of heat fluxes in addition to temperatures.

For SWIR STM only, the disturbance of the thermo-couples must be taken into account because they create parasitic couplings between cold parts and room environment even if special care is done to reduce this effect: thermal loop, K type thermo-couple with insulating metals instead of copper. The influence of each thermo-couple is evaluated taking into account the conduction and the radiative exchange. This correction is unneglectable and represents 3.5°C.

Thermal Results

After corrections presented here above, the thermal performances of SWIR and VNIR FPAs are validated:

- the detectors can be cooled down to the specified temperature with the allocated power;
- for VNIR, the model of the TEC correctly simulate the relationship between the temperature of the detector and the applied current and the associated power rejected;
- for SWIR, the power needed to maintain the temperature of the detector between hot and cold is 2.13W that is less than expected. In addition, margin is very low in hot case.

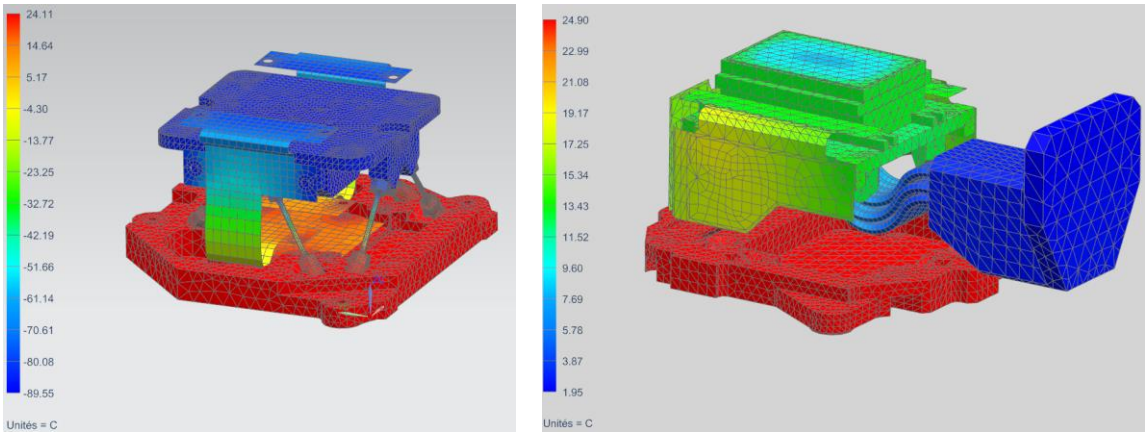

SWIR FPA VNIR FPA

Figure 17: Thermal gradients in FPAs for cold case.

CONCLUSION

The design of the SWIR and VNIR FPAs for the 3MI instrument is a challenging tasks because each of the parts is the result of a sharp compromise between thermal, mechanical (thermo-elastic and dynamic), geometrical interfaces and, sometimes electrical requirements.

Most of the performances, thermal insulation, stiffness and stability, are achieved by the help of an ISM based on a hexapod composed of titanium shafts. Even if these shafts look fragile, they can withstand important loads because they work in tensile and compressive direction. The design of the thermal strap is also a key point in terms of flexibility, thermal resistance and integration into the FPA volume and connection with the mechanical parts.

Even if it doesn't directly link to the performances, the lack of space is a great design constrain because any modification of the position of an item will affected the other ones. The size of the detector in comparison to the volume allocated in the IRD and the relative position of the cold sink interface are some examples of encountered difficulties.

Ideally, the global architecture of the FPA should be circular centered on the optical axis. In this sense, the presented FPAs reach this optimum with the hexapod but thermal strap aperture and electronic connections should be reserved: thermal strap aperture located at the center of the baseplate and the electronic connections on the edges.

A more generic approach for the design of the ISM can be the topologic optimization to find or to guide to the best design according to thermal, mechanical and geometrical specifications. This approach will only be valid until 3D printing manufacturing will be fully qualified in space applications.

REFERENCES

[1] ESA, "MetOp-SG (MetOp-Second Generation Program)," https://earth.esa.int/web/eoportal/satellite-missions/m/metop-sg
[2] Daniele Biron, Angelo Lupi, Giorgia Montini, Demetrio Labate, Umberto Bruno, Davide Melfi, Massimiliano Sist, Francesco Zauli, Luigi De Leonibus, "METOP-SG 3MI (Multi-viewing Multi-channel Multi-polarization Imaging), a powerful observing mission for future operational applications,"
[3] ESA, "Thermal control general Requirements - ECSS-E-ST-31C", (2008)
[4] AIRBUS DEFENSE & SPACE, "MetOp-SG, Instrument General Design and Interface Requirements (INS GDIR)", (2014)
[5] Lucie Jamot, Émilien Carrié, "Feedback from a space optronic supplier on shocks", Proc. ECSSMET 2018
[6] Wright G. S., Rieke G. H., Colina L., van Dishoech E., Goodson G., Greene T., Lagage P. O., Karnik A., Lambros S. D., Lemke D., Meixner M., Nørgaard-Nielsen Hans Ulrik, Oloffson G., Ray T., Ressler M., Waelkens C., Wright D., Zehnder A., "The JWST MIRI instrument concept", Proceedings of SPIE - The International Society for Optical Engineering, (October 2004)
[7] ESA, "EUCLID – Definition Study Report", (July 2011)
[8] Michael Borden, Derek Lewis, Hared Ochoa, Laura Jones-Wilson, Sara Susca, Michael Porter, Richard Massey, Paul Clark, Barth Netterfield, "Thermal, Structural, and Optical Analysis of a Balloon-Based Imaging System", Astronomical Society of the Pacific, (March 2017)
[9] ESA, "Buckling of structures - ECSS-HB-32-24A", (March 2010)
[10] Adam L. Woodcraft, "Predicting the thermal conductivity of aluminium alloys in the cryogenic to room temperature range", Cryogenics 45 (6), p. 421-431, (2005)